Heritage Science

RESEARCH ARTICLE

Evaluation of polyvinyl alcohol–borax/agarose (PVA–B/AG) blend hydrogels for removal of deteriorated consolidants from ancient Egyptian wall paintings

Ehab Al-Emam[1,3]* , Abdel Ghafour Motawea[2], Koen Janssens[3] and Joost Caen[4]

Abstract

This study concerns the assessment of a new polyvinyl alcohol–borax/agarose blend hydrogel (PVA–B/AG) tailored for the conservation of ancient Egyptian wall paintings. The increasing problems of deteriorated consolidants affecting ancient wall paintings have attracted the interest of conservation scientists in the last 20 years. The ability of a new blend for removing aged Paraloid® B-72 layers from painted stone and plaster samples has been evaluated. The hydrogel blend was used to expose the aged Paraloid in a controlled manner to six different cleaning system (CS). CS1–CS4 consist of solvents or solvent mixtures; CS5 and CS6 are nanostructured fluids (NSFs). The evaluation of the removal process was carried out by quantitative and qualitative methods, namely, visual examination, 3D microscopy, contact angle and colorimetric measurements and by Fourier transform infra-red spectrometry in reflectance mode. The results showed that the PVA–B/AG blend hydrogel, loaded with specific cleaning systems, was able to remove deteriorated B-72 and allowed to restore the painted surface to a state close to the original one. The PVA–B/AG blend showed good workability, permitting it to be easily cut, shaped, applied and removed. It could also be verified by means of different investigation methods that the blend left no detectable residues. As a final realistic check of the method, the PVA–B/AG hydrogel loaded with the best functioning cleaning system (CS3) was used to remove an aged consolidant layer from an ancient Egyptian wall painting.

Keywords: 3D Microscope, Hydrogels, Color measurement, Contact angle, Egyptian wall paintings, Paraloid® B72, Polyvinyl alcohol–borax/agarose blend, r-FTIR

Introduction

Wall paintings represent an important part of cultural heritage artefacts as they convey information on the life of our ancestors as well as their technologies. They are complex works of art because of their stratigraphy and variable inorganic and organic components [1, 2]. Over time, they are susceptible to degradation due to different external influences such as temperature, moisture, salts, light, micro-organisms etc. Those agents can trigger multiple deterioration mechanisms, resulting in damage to one or more strata of the wall painting. One of the most common visible results of the degradation of archaeological wall paintings is loss of internal cohesion among the layers as well as powdering of pigments due to deterioration of the binder [3, 4].

In such situations, conservators usually consolidate the fragile layers to halt pigment losses. For years (and up to the present time), synthetic polymeric materials are widely preferred by conservators for consolidating fragile pictorial layers since the reinforcing of weak preparatory layers can be combined with protecting the surface from water penetration [5, 6]. On the other hand, on many archaeological surfaces that were treated, several drawbacks of their use have become apparent over the years:

*Correspondence: ehab.al-emam@uantwerpen.be;
ehab_alemam@art.sohag.edu.eg
[1] Department of Conservation, Faculty of Archaeology, Sohag University, Sohag 82524, Egypt
Full list of author information is available at the end of the article

Al-Emam *et al. Herit Sci*   (2019) 7:22

Page 2 of 18

(a) the polymers cause changes to the optical appearance of a wall painting due to their high refractive index [7]; (b) they may produce color alterations and glossy surfaces especially when applied in high concentration; (c) due to chemical breakdown of the consolidant material itself, it may yellow and/or darken; (d) the consolidated surfaces have the tendency to entrap airborne particulate matters [8]; (e) these organic polymers give rise to physiochemical alterations of the surface they were applied on as they are hydrophobic and incompatible with inorganic porous surfaces [9, 10].

The aforementioned drawbacks emphasized the problems associated with the removal of these consolidants. An important aspect is the so-called reversibility of the polymers. Two points should be considered when discussing this: (a) the solubility of these materials is influenced by ageing and the solvents become less effective vs time (e.g., aged soluble nylon [11]); (b) the application process of these materials is irreversible when they are applied on a porous surface; in this case it is difficult to extract the polymer completely from the bulk of the work of art [12].

Already in the 1980s, microemulsions were used for the removal of hydrophobic coatings from frescoes in the Brancacci Chapel, Italy. Since then, microemulsions and micellar systems were extensively investigated and employed for removing deteriorated synthetic materials from architectural surfaces [13–15]. In the past, these cleaning systems were usually delivered to the surface under treatment by means of cellulose pulp. Thereafter, gels were used as carriers for microemulsions and solvents for the sake of controlled application and selective removal of the polymeric materials [16–19].

In the same context, high viscous polymeric dispersions (HVPDs), based on polyvinyl alcohol crosslinked with a borax (PVA–B), were developed for the cleaning of works of art. They are gel-like materials as they cannot be considered gels from a rheological point of view [20–22]. Initially, fully hydrolyzed PVA–B systems were investigated in the conservation field [23, 24]. The consistency of these highly elastic viscous systems can be modulated via changing the molecular weight of PVA polymer and the concentration of PVA and borax in addition to the pH and temperature of the aqueous solution [25]. Later, using partially hydrolyzed poly(vinyl acetate)–borax permitted the incorporation of a wider range of organic solvents in larger concentrations [18, 26]. The abovementioned systems are characterized by ease application and removal from the treated surface using tweezers without further use of solvents, which is the case of solvent gels [20, 27]. It was also possible to prepare organogels from partially hydrolyzed poly(vinyl acetate) by using benzene-1,4-diboronic acid as a crosslinker and dissolving them in the following organic solvents: dimethyl sulfoxide, dimethylformamide, tetrahydrofuran, 2-ethoxyethanol, and methanol [28]. Furthermore, obtaining hydrogels from PVA polymers by freeze–thaw cycles was investigated. The resulting hydrogels were loaded with oil-in-water microemulsions and they were effective in removing hydrophobic grime [29, 30]. Recently, other studies attempted to improve the characteristics of PVA–B by blending it with polyethylene oxide polymer. Polyethylene oxide improved the liquid retention of PVA–B as well as the ability to maintain its shape [31, 32].

In our preliminary tests on PVA–B, it was noticed that it sometimes flows over the treated surface during long contact time applications [21]. In addition, the fact that PVA hydrogel is flexible, viscous, and has a slimy consistency makes it difficult to be cut and formed in specific shapes for selective application on a complex surface. This led to the idea of blending PVA–B hydrogel with agarose (AG) hydrogel, which is a much more rigid material. Blending PVA with polysaccharide hydrogels has been reported in several studies related to pharmaceutical and biomedical applications. It has been noted that these polysaccharide hydrogels improve the mechanical properties of PVA hydrogels [33–36].

The complete characterization of the hydrogel is not in the scope of this paper but will be investigated in a later study. In the first place, we aimed to test the efficiency of the new PVA–B/AG blend hydrogel as a realistically applicable cleaning tool for wall paintings by performing a number of cleaning efficiency tests in the lab. Secondly, the blend has been tested in the conservation of ancient Egyptian wall paintings, affected by deteriorated polymeric consolidants. In addition, we wanted to investigate the following features: (a) the ease of shaping of the hydrogel to suit the selective cleaning of consolidated parts of wall paintings, (b) if it is flexible enough to adapt to the 3D form of reliefs, (c) its ability to retain the liquids at elevated temperatures above 35 °C as in the case of most of the Egyptian archaeological sites, and (d) its shape stability in long contact time applications.

Therefore, the hydrogel was loaded with cleaning systems composed of different solvents and nanostructured fluids tailored for dissolving Paraloid® B-72. Paraloid® B-72 is the commonly preferred polymer by conservators for the conservation of paint layers because of its stability over other synthetic polymers [37]. A PVA–B/AG ratio of 3:1 was used, based on pre-tests aimed at obtaining a blend with suitable workability. Painted mock-up samples were consolidated with Paraloid® B-72, artificially aged and then treated with PVA–B/AG blend loaded with six different cleaning systems. The removal efficiency was evaluated through several qualitative and quantitative methods, allowing the ranking of the cleaning systems.

Al-Emam *et al. Herit Sci*   (2019) 7:22

Page 3 of 18

We also investigated the treated samples for the presence of PVA−B/AG residues. Finally, as a test of the method in realistic conditions, the most effective cleaning system was loaded in the PVA−B/AG blend hydrogel and employed in situ on an ancient Egyptian wall painting (see "Field tests" section).

Materials and methods

Materials

Polyvinyl alcohol (*PVA*) (98.0–98.8% hydrolyzed, M.W. 146,000–186,000-Acros Organics). Agarose (*AG*) from Sigma-Aldrich. Di-Sodium tetraborate decahydrate (*borax*) (ACS, ISO reagent, Merck). Paraloid® B72 (*B-72*) pellets (ethyl-methacrylate copolymer, Kremer pigmente). 1-Butanol (*1-BuOH*) (ACS, ISO reagent, Merck). Acetone (*AC*) (purity ≥ 99.8%, VWR PROLABO). *N,N*-Dimethylformamide (*DMF*) from Janssen Chimica. Methyl ethyl ketone (*MEK*) (technical, VWR PRO-LABO). 1-Pentanol (*1-PeOH*) (purity > 99.0%, M.W. 88.15, TCI). Propylene carbonate (*PC*) (purity 99%, Alfa Aesar). Ethyl acetate (*EA*) (HPLC, LAB-SCAN Analytical Sciences). Sodium dodecyl sulfate (*SDS*) (purity 98%, Sigma-Aldrich). Laboratory stretch film (Dura Seal™). Red Moroccan ochre, fine (Kremer pigmente). Bone glue in pearls (Deffner and Johann).

Sample preparation

Two types of wall painting mockup samples of different porosity were prepared to evaluate the behavior of the PVA−B/AG blend. The first type consisted of limestone tiles (∼ 7.5 × 5 × 0.8 cm) that were painted with two layers of finely ground red ochre; bone glue was used as binder. After a week, the painted tiles were brushed with three layers of B-72 5% dissolved in acetone 90% and DMF 5% (w/v). The second type of samples consisted of plaster tiles, composed of slaked lime, sieved sand (less than 600 μm), and gypsum. They were mixed together well with deionized water in 1:1:0.5:0.5 volume ratios respectively. Then the mixture was poured/pressed into a mold to obtain a plaster slab with homogeneous porosity. The plaster slabs were cut into tiles of the same dimensions as the limestone ones and left to dry for 15 days. These plaster tiles were covered with a thin limewash layer and then painted with five layers of red ochre/bone glue paint. Finally, they were consolidated with the same B-72 5% solution as above. The open porosity of the limestone and plaster tiles were measured via water absorption by total immersion [38, 39]. The open porosity of the stone tiles was 31% while that of the plaster tiles was 46%.

Artificial accelerated ageing

Artificial accelerated ageing was executed in a (BAM-Global-UV-Testgerät Model UV 200 RB/20 DU (System Weiss) machine. The samples were exposed to a temperature at 70 °C, relative humidity of 50% [40] in addition to light illumination for 250 h. The climatic chamber is operated with 18 fluorescent lamps (Philips, Actinic BL TL 40W/10 SLV/25), providing ultraviolet light in the UV-A range (400–320 nm). The illuminance was 1250 ± 210 lx, as measured using a Skye Lux sensor SKL310 (sensitivity: 0.1 mV/kLux). The value of the UV-A irradiance was measured to be 31.5 ± 2.6 W/m^2, obtained by using a Skye UVA SKU421 sensor with calibrated sensitivity (0.055 W/m^2/mV).

Afterwards, the samples were exposed to 70 °C temperature for 2 h and left for 3 days at room temperature before the B-72 removal test. The samples showed darkening due to the degradation of B-72 layer after the ageing.

PVA−B/AG blend hydrogel preparation

A stock solution of 10% of PVA was prepared in distilled water (w/v) at 100 °C under reflux using a magnetic stirrer until a clear solution was obtained. In addition, borax was dissolved in distilled water to prepare a 6% (w/v) stock solution; heat was used to speed up the dissolving process. It is worth mentioning that the borax stock solution should be stirred prior to every use to re-dissolve the precipitated particles. PVA−B/AG blend hydrogel was prepared with the following concentrations (w/v): 3% of PVA, 1% of AG, and 0.6% of borax in addition to the proper concentration of the cleaning system (*CS1−CS6*) (Tables 1 and 2). The 1% AG concentration provides a sufficient degree of rigidity to the blend without losing its flexibility. Blends with higher AG concentration show the rigidity of the agarose hydrogels while lower AG concentration leads to blends with more pronounced PVA hydrogels features. The selection of solvents and solvent mixtures listed in (Table 1) was based on their potential B-72 dissolution power on the Teas diagram [12]; they were pre-tested prior their incorporation into the hydrogel. Furthermore, two nanostructured fluids (NSFs) were included in the experiment to evaluate the possibility of their incorporation into the hydrogel in addition to their efficiency in removing B-72. The first NSF was the so-called EAPC system which is mainly composed of the two partially dissolved solvents: ethyl acetate (EA) and propylene carbonate (PC). In addition, it includes 1-pentanol (1-PeOH) as a co-surfactant, SDS as a surfactant, and water. This system was proven to be effective for the removal of polymers [41]. The second NSF was based on a ternary system composed of MEK, a surfactant, and water. The performance of this system in swelling and removing B-72 polymer from glass and lime-based surfaces was tested. The system yielded excellent removal performance in particular when a nonionic

Al-Emam *et al. Herit Sci*   (2019) 7:22

Page 4 of 18
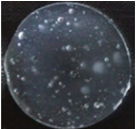
Table 1 Components and physical appearance of the hydrogels (w/v)
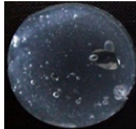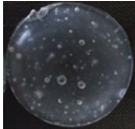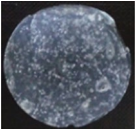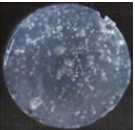
Reagents	CS1	CS2	CS3	CS4	CS5	CS6
PVA	3%	3%	3%	3%	3%	3%
AG	1%	1%	1%	1%	1%	1%
Borax	0.6%	0.6%	0.6%	0.6%	0.6%	0.6%
Water	70.4%	70.4%	75.4%	75.4%	70.4%	70.4%
AC	25%	15%	–	–	–	–
1-BuOH	–	10%	–	10%	–	–
MEK	–	–	10%	–	–	–
1-PeOH	–	–	10%	–	–	–
EA	–	–	–	10%	–	–
EAPC (NSF)	–	–	–	–	25%	–
MEK1-PeOH (NSF)	–	–	–	–	–	25%
Physical appearance of hydrogels on a black background						

Table 2 Components of the nanostructured fluids incorporated in the hydrogels (w/w)

Reagents	EAPC (NSF) (%)	MEK1-PeOH (NSF) (%)
SDS	3.7	3.5
1-PeOH	7	10
EA	8	–
PC	8	–
MEK	–	20
Water	73.3	66.5

surfactant was used [40, 42, 43]. The mechanism of this system in removing B-72 from glass slides was explained by Raudino et al. [43]. First, water causes structural reorganization of the outer part of the polymer and then the organic solvent swells the external part of the polymer. Meanwhile, the surfactant works on the detachment of the swollen polymer layer via decreasing the surface tension at the glass/polymer interface. Based on our preliminary tests, we added 1-PeOH to this system because we noticed good removal of B-72 when it was blended with MEK; we referred to this system as (MEK1-PeOH) (Table 2). The two NSFs were prepared separately as clear solutions and then were loaded into the hydrogel. The highest concentration of the abovementioned NSFs that could be loaded into the PVA–B/AG hydrogel was 25% as higher concentrations caused severe syneresis (liquid escaping from the gel surface) due to SDS.

In general, the addition of AG to PVA–B system causes some turbidity in the resulting hydrogel. The physical appearance of the prepared hydrogels was different due to the incorporated solvents and their concentration. Angelova et al. [21] noticed the formation of two-phase system after incorporating 1/1 water/1-PeOH into PVA–B. The system was opaque and underwent syneresis within minutes to hours. In our case, no considerable syneresis in CS3 was observed and this may be due to the lower concentration of 1-PeOH used (10%). However, different degrees of whitish appearance were observed in the cleaning systems containing 1-PeOH (CS3, CS5, and CS6). This could be because of the low miscibility of 1-PeOH in water (22 g/L). As a simple test, a whitish solution was obtained upon stirring 10% of 1-PeOH in water without the presence of PVA or AG polymers. The same observation, but lesser, can be seen in CS2 and CS4 loaded with 10% 1-BuOH whose solubility is 66 g/L (Table 1). The other solvents have less effect on the appearance owing to their better solubility in water (AC: miscible; PC: miscible; EA: 85.3 g/L; MEK: ~ 100 g/L).

Practically, in order to prepare 10 ml of the blend hydrogel loaded with CS1, 3 ml of 10% PVA stock solution was stirred on a hot plate with 0.1 g of AG and 3.4 ml of distilled water at 80 °C for c. 15 min until the agarose was fully dissolved and a clear solution was obtained. Then the solution was left to cool down (45–50 °C) and afterwards 2.5 ml of acetone was added to the solution while stirring. Finally, 1 ml of the 6% borax stock solution was added dropwise under vortex mixing to form the hydrogel and further mixing with a spatula was sometimes be necessary to ensure that the borax reached the

Al-Emam *et al. Herit Sci*   (2019) 7:22

Page 5 of 18

whole PVA polymer. The hydrogel should be introduced rapidly into the mold with a spatula and left to cool and relax for c. 30 min. For faster preparation, a microwave oven can be used to dissolve the agarose in a few seconds [44, 45]. Later, the hydrogel is kept in a refrigerator for 1 day before use. In order to obtain a flat gel surface unmarked by air bubbles, it is recommended to flip over the hydrogel piece in the mold several times using tweezers.

B-72 removal protocol

Using a spatula, a piece of hydrogel (c. 2 × 2 cm with a thickness of 2 mm) was cut and applied on the sample surface after which it was gently pressed to ensure full contact with the surface and take its structure. The hydrogel piece was covered with Dura Seal™ film to hinder the evaporation of the liquids. The hydrogels loaded with NSFs were wiped with a clean tissue before application to remove any extra liquids escaping from the hydrogel (syneresis). It is worth mentioning that empirical removal tests were done to determine the appropriate contact time. In these tests, we started with 1 h of contact time but this proved to be insufficient to dissolve the B-72, causing damage to the paint layer during dry cotton swab clearance with a gentle rotating motion. This feature was very clear in the case

of CS2. Hence, we adopted 3 h of contact time for the solvent cleaning systems and 5 h for the NSFs because they required more time to show results. The hydrogel pieces were removed by means of forceps after which the residual B-72 solution was cleared with a dry cotton swab (Fig. 1a). It is important to clear the surface directly after removing the hydrogel in order to avoid a drying residual of dissolved B-72. This can be done by lifting the hydrogel piece gradually and clearing the exposed part.

Six painted stone and six painted plaster samples were treated by means of each cleaning system. Generally speaking, the PVA–B/AG blend hydrogel was able to deliver the cleaning systems consistently to the painted surfaces. Additionally, it was easy to be cut and shaped as desired as well as being easy to apply and remove from the painted surface. It has the ability to be applied on vertical surfaces which is crucial in case of wall paintings conservation (Fig. 1d).

In case of the NSFs, the hydrogel sometimes adhered to the surface of the plaster samples, leaving a thin layer of the hydrogel. This may be attributed to two phenomena: firstly, the liquids of the hydrogel piece dried out because of the high porosity of the plaster as well as the long contact time (5 h). This hydrogel dryness occurred especially at the interface with the sample surface. Secondly, the
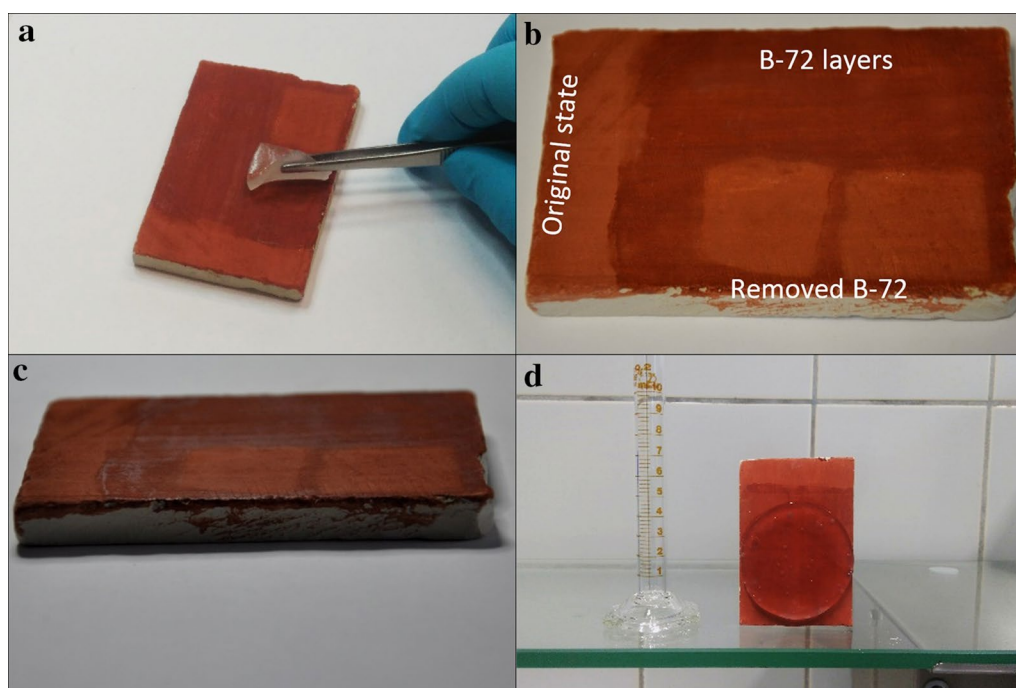

Fig. 1 **a** Removing the hydrogel piece easily by means of forceps. **b** Removed B-72 from two areas by CS3. **c** The same sample under raking light reveals the restored matte appearance of the treated areas. **d** Illustrates the ability of shaping the PVA–B/AG blend hydrogel and the ease of application in the vertical position

Al-Emam *et al. Herit Sci*   (2019) 7:22

Page 6 of 18

dissolved B-72 can also dry and cause the adherence of the hydrogel to the painted plaster.

Evaluation of B-72 removal efficiency

In the specialized literature, there are no descriptions of fixed methods for evaluating the removal efficiency of old consolidants and varnishes from artwork surfaces. Normally, visual examination is the most common and easiest method of assessing the removal of the deteriorated polymer by the confirmation of the restoration of the original surface optical properties. However, this is not a satisfactory method because the same result may be interpreted differently by different individuals. Hence, it is better to accompany visual examination by microscopic examinations (by optical and scanning electron microscopes) and analytical techniques such as FTIR spectroscopy to verify the results [19, 24, 46, 47]. Since the process implies the removal of a hydrophobic material from a porous surface, some studies employed methods to measure the wettability of the surface before and after the treatment. In these studies, either the contact angle of a water drop at the surface, the capillary absorption, or the water vapor permeability [40, 48–50] were measured. In other studies, the decrease of the polymer/varnish layer thickness could be measured by optical coherence topography (OCT) or by means of a 3D microscope [51, 52].

In our study, we aim to evaluate the efficiency of the six cleaning systems for B-72 removal from porous surfaces. Hence, we adopted several qualitative and quantitative methods to allow us to: (a) Reach a definite decision concerning the best cleaning system. (b) Arrive at an integral evaluation of these methods that pinpoints the possible limitations of some of them [51]. (c) Evaluate the different aspects of the treated surface with the cleaning systems (i.e. optical appearance, chemical composition, and wettability).

The selected evaluating methods were as follows: (i) visual examination, (ii) colorimetric measurements, (iii) contact angle measurements, (iv) reflectance FTIR spectrometry, and (v) 3D microscopy. The data of the quantitative methods were processed by comparing the results after B-72 removal to those before the removal according to (Formula 1) where *I* represents the measured property such as color difference (ΔE*), contact angle (CA), FTIR intensity, and relative thickness of B-72 layer [53]. The higher the relative change, the better the removal efficiency.

$$B\text{-}72\ removal\ efficiency$$
$$= \frac{I\left(Before\ removal\right) - I\left(After\ removal\right)}{I\left(Before\ removal\right)} \times 100\%$$

(1)

Instrumentations and measurements
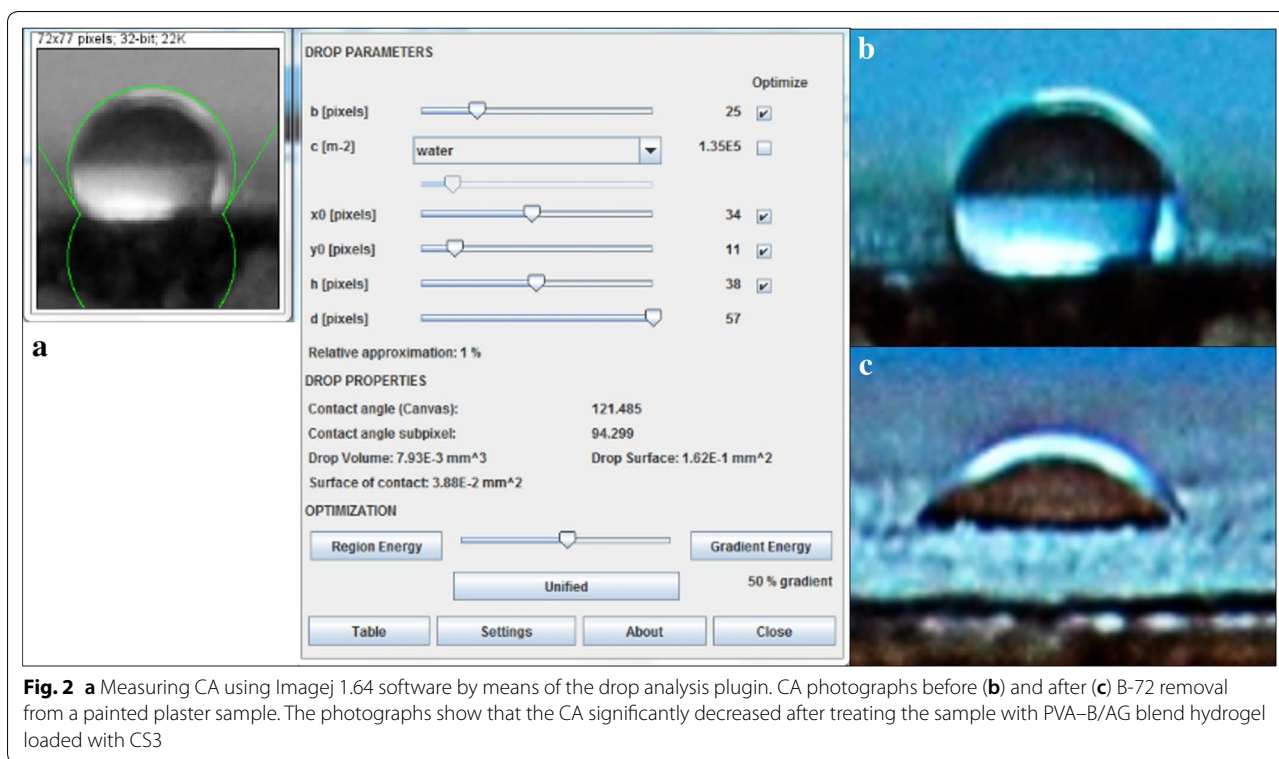#### Colorimetric measurements

The color measurements were undertaken by an AvaSpec-2048 fiber optic spectrometer equipped with the tungsten halogen light source AvaLight-Hal (360–2500 nm). The reflected radiation was analyzed by the software AvaSoft 7.5. The CIE Lab values were recorded using the standard illuminant D65 and the 2° standard observer. These measurements were collected from the original surface (unconsolidated), in addition to before and after B-72 removal. The collected CIE Lab values represented the average of five measurements of a treated sample and then the color difference (ΔE*) value was obtained according to CIE 1976. The ΔE* of each cleaning system was calculated based on the average of three measured samples. Finally, the efficiency was calculated based on the (Formula 1).

Contact angle measurements (CA)

Static contact angle measurements reflect the hydrophobicity of consolidated porous surfaces [54]. The CA measurements were carried out according the standard UNI EN 15802:2010 by constructing a simple goniometer. A micropipette was used to deliver a 5 μl drop of distilled water to the sample surface and captured using a Nikon D90 digital camera within 5 s. The obtained images were processed in the Imagej 1.64 software using the drop analysis plugin. The average of CA of five water drops were measured for the sample surface before and after B-72 removal. Afterwards, the efficiency of B-72 removal was calculated according to (Formula 1). For each cleaning system, these measurements were performed on three treated samples and the average of them was collected to obtain a representative result. The temperature and relative humidity were approximately 21 °C and 34%, respectively, during the measurements. A larger decrease in CA values indicates a higher efficiency of the cleaning system (Fig. 2).

Reflectance FTIR spectrometer (r-FTIR)

IR spectra were collected from the sample surfaces using a Bruker ALPHA-R FTIR spectrometer in reflection mode. The scans were measured in the mid-infrared (MIR) region (4000–375 cm^{-1}) with a spectral resolution of 4 cm^{-1}. The samples were positioned in front of the spectrometer at a distance of around 1.5 cm; the diameter of the focal spot was approximately 2 mm. The built-in video camera was used to target the desired spot on the sample surface. Each spectrum represents the average of 5 min data acquisition to improve the signal-to-scan ratio. Five measurements were recorded for each cleaning system before and after B-72 removal and then compared with the spectrum of the original surface. Furthermore,

Fig. 2 a Measuring CA using Imagej 1.64 software by means of the drop analysis plugin. CA photographs before (**b**) and after (**c**) B-72 removal from a painted plaster sample. The photographs show that the CA significantly decreased after treating the sample with PVA–B/AG blend hydrogel loaded with CS3

this technique was employed to determine the possibility of residual hydrogel left on the treated samples.

3D microscope

The samples were examined after the B-72 removal process using an Olympus Digital Microscope DSX510. It was employed to detect the removal efficiency of B-72 by the six cleaning systems loaded into PVA–B/AG blend hydrogel, in addition to the presence of hydrogel residues on the treated surfaces. Furthermore, this technique was employed to give quantitative data by measuring the relative thickness of the B-72 layer before and after the treatment. All the pictures were acquired in 3D mode using an XLMPLFLN10XDSX objective lens (10×) with a total magnification of 300×. The profile 3D measurement tool was used to obtain the decrease in the relative thickness of B-72 after the treatment. The six cleaning systems loaded into the PVA–B/AG hydrogel were used to remove the B-72 coating from a chosen painted stone sample. The reason for that was to make sure that the B-72 layer have the same height for better evaluation. Due to the surface roughness, the average of thirty measurements (ten measurements on three different spots) was calculated for each cleaning system and compared to those before the treatment; the efficiency of removal was then calculated on the basis of these averages.

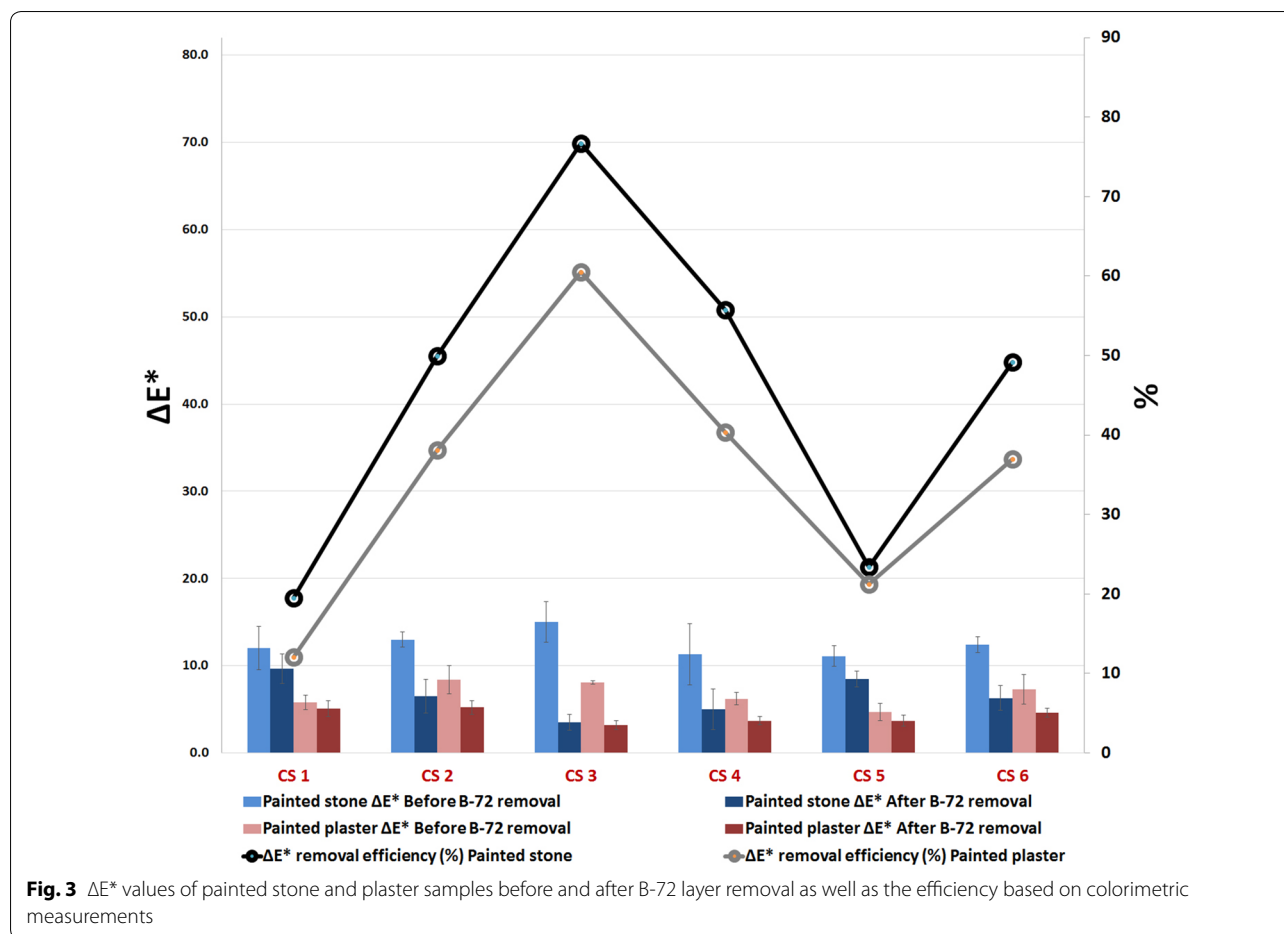## Results and discussions

Visual examination

By examining the treated samples visually, it became clear that the hydrogels loaded with the solvent cleaning systems CS2, CS3, and CS4 removed the B-72 layer better than the other cleaning systems. Under raking light, the visual appearance of the surfaces treated with CS3 is the closest to that of the original surface (Fig. 1b, c). NSFs cleaning systems CS5 and CS6 were less effective than CS2–CS4; CS1 (acetone 25%) caused no changes to the treated surfaces.

Colorimetric measurements

The ΔE^* values decreased after the removal of the B-72 layer; a significant decrease of ΔE^* value could be obtained by means of CS3, followed by CS4 (Fig. 3). In addition, CS2 and CS6 are ranked as the third and fourth effective cleaning systems respectively. Both CS1 and CS5 gave a slight deascrease to ΔE^* values which is indicative of their low efficiency in B-72 removal from the painted surface.

CA measurements

For all cleaning systems, the decrease of CA in the painted plaster was larger than that in the painted stone. This may be attributed to the high porosity of the painted plaster samples which caused more diffusion of the B-72

Fig. 3 ΔE* values of painted stone and plaster samples before and after B-72 layer removal as well as the efficiency based on colorimetric measurements
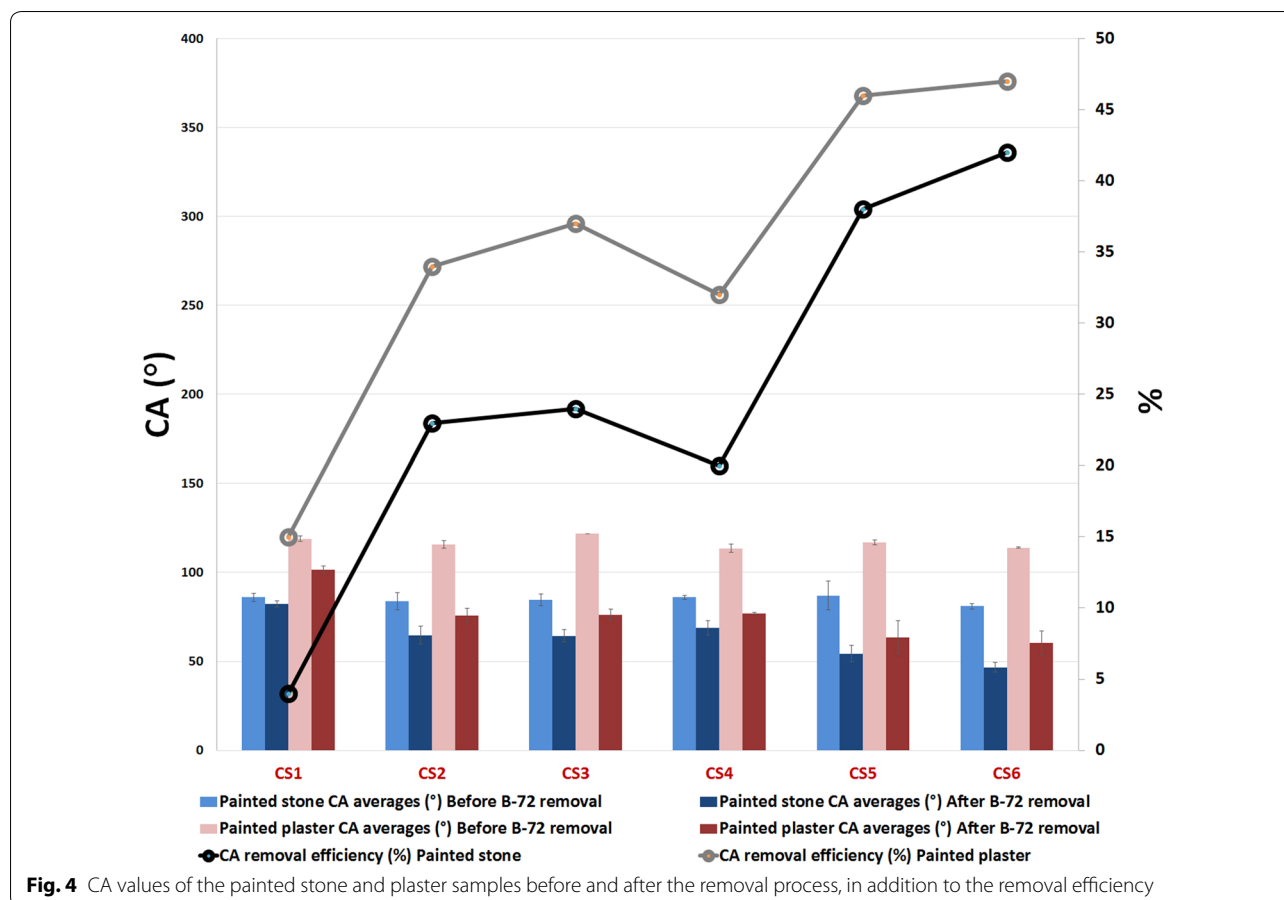
layer into the bulk of the sample. Among CS1-CS4, CS3 shows a more noticeable decline in measured CA than CS2 and CS4 respectively (Fig. 4). In the case of CS1, the smallest effect on the CA was observed, suggesting CS1 is the least effective cleaning system in dissolving B-72.

Use of CS5 and CS6 caused dramatic decreases in CA which might suggest that they were able to remove the hydrophobic B-72 layer and restore the permeability of the painted surface. Since CS5 and CS6 contain NSFs, it cannot be excluded that the surfactant (SDS) influenced the surface tension of the delivered water drop and thus interfered with the CA measurements. To investigate this hypothesis, an additional test was implemented in which a consolidated painted plaster sample was treated with a solution of 1% SDS in distilled water using a cotton swab. Then the surface was cleared with a cotton swab imbedded in distilled water three times. The CA decreased by 44% after treating the surface with SDS solution even in the presence of the B-72 layer on the sample surface. Consequently, it can be concluded that CA measurements of CS5 and CS6 are not useful to estimate B-72 removal efficiency; thus they were omitted from the evaluation.

r-FTIR

The FTIR analyses were focused on the painted stone samples that showed meaningful difference in spectral response before and after B-72 removal. This was not the case for the painted plaster samples, probably because of the higher roughness of the surface. The spectra of the original (unconsolidated) stone samples feature the typical peaks of red ochre (Fig. 5). Quartz is identified by the presence of peaks at 1041 (Si–O–Si), 791, 774, and 693 cm^{-1} while the peaks at 542 and 472 cm^{-1} are attributed to iron oxide (hematite) [55]. In addition, kaolinite is present through the peaks 1009 (Si–O–Al), 927 cm^{-1}, and 909 cm^{-1} (Al–O–H) [56, 57]. On the other hand, the analyzed samples before the removal of B-72 layer show a distinctive peak at 1717 cm^{-1} of ester carbonyl C=O stretching and the peaks at 1458 and 1375 cm^{-1} are indicative for the antisymmetric and symmetric bending of the α-methyl group CH$_3$. The peak around 1230 cm^{-1} reveals the presences of C–O ester stretching while the intense two peaks at 1164 and 1136 cm^{-1} are attributed the C–C(=O)–O antisymmetric stretching. The peak that appears around 1017 cm^{-1} is assigned to O–C–C
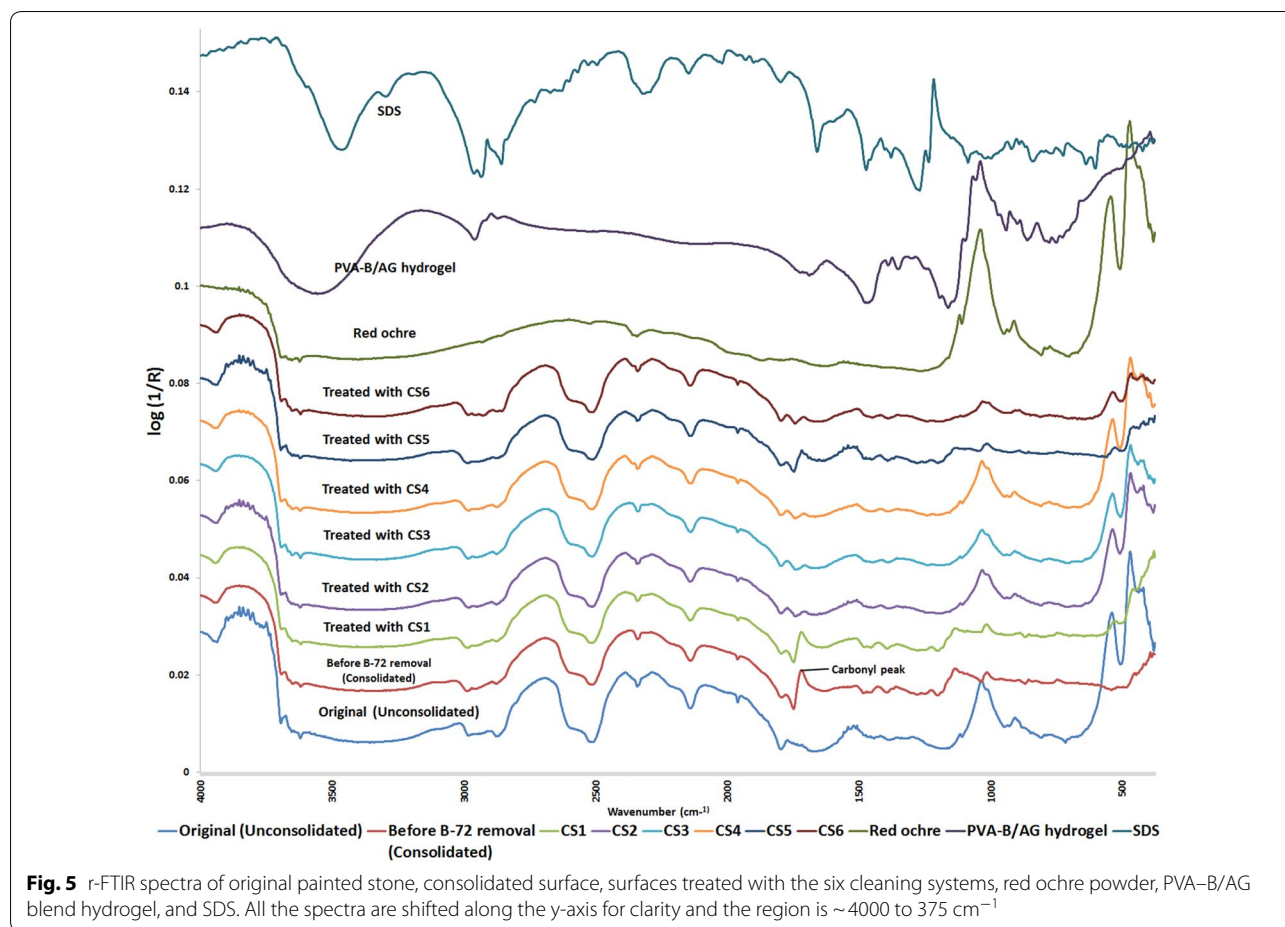
Fig. 4 CA values of the painted stone and plaster samples before and after the removal process, in addition to the removal efficiency

stretching of the ethyl ester. Additionally, the bands at 854 and 746 cm^{-1} are characteristic of the $-CH_2-$ rocking [58–60]. It can be noticed that the red ochre peaks are masked by the B-72 peaks in the consolidated samples.

The spectra of the analyzed surfaces after B-72 removal reflect some remarkable features. Firstly, the distinctive peak of the carbonyl group at ~1717 cm^{-1} decreases in intensity. Secondly, the red ochre peaks around 1041, 791, 774, 693, 542, and 472 cm^{-1} re-appeared after they were masked by the presence of the B-72 layer. The decline of the carbonyl peak was used to estimate the amount of B-72 left on the cleaned surfaces and consequently the removal efficiency of the six cleaning systems. The ratio of height/area of the carbonyl peak to that of the calcite peak at ~2510 cm^{-1} was calculated for the spectra of samples treated with each cleaning system as well as the surface before B-72 removal. The average ratio of five spectra per treatment was obtained. The removal efficiency was calculated by applying (Formula 1) to the aforementioned ratio values of the six cleaning systems (Fig. 6). According to the estimates of the removal efficiency, the most effective cleaning systems were CS3,

CS2, and CS4 respectively. The NSFs (CS5 and CS6) were less effective and CS1 was the least effective.

Regarding the detection of the presence of PVA–B/AG blend and SDS residues after the treatment, both materials were analyzed FTIR. The FTIR spectrum of PVA–B/AG blend features a band around 3500 cm^{-1} which is attributed to O–H stretching vibration from the hydroxyl groups and hydrogen bonds. The peak around 2922 cm^{-1} is associated to CH stretching of the CH_2 group. The peaks at 1400 and 1320 cm^{-1} demonstrate the asymmetric stretching of B–O–C which indicate the crosslinking of PVA with borax via didiol complexation [61]. The band at 828 cm^{-1} is assigned to the B–O stretching vibration from residual $B(OH)_4$ [62]. On the other hand, the IR bands at ~1150 and 1070 cm^{-1} represent the –C–O–C– and glycosidic linkage while those at 927, 890, and 767 cm^{-1} are associated with 3,6-anhydrogalactose unit of the agarose [63]. The SDS spectrum shows the asymmetric and symmetric CH_3 stretching vibrational frequencies at 2951 and 2881 cm^{-1} while the asymmetric and symmetric CH_2 stretching vibrational frequencies are located at 2914 and 2846 cm^{-1}. The characteristic

Fig. 5 r-FTIR spectra of original painted stone, consolidated surface, surfaces treated with the six cleaning systems, red ochre powder, PVA–B/AG blend hydrogel, and SDS. All the spectra are shifted along the y-axis for clarity and the region is ~4000 to 375 cm^{-1}

intense double band at 1215 and 1246 cm^{-1} is attributed to SO$_2$ stretching [64].

3D microscopy

The photographs/height maps obtained by the 3D microscopy show results that coincide with those of the previous evaluation methods (Figs. 7 and 8). B-72 residues were hardly detectable in the samples treated with PVA–B/AG hydrogel loaded with CS3. A minor amount of B-72 was present in the case of CS2 and CS4. The NSFs provided less removal efficiency while the B-72 layer was still obvious on the surface of the samples treated with CS1. The same results were given by the collected measurements of the relative B-72 thickness of the consolidated painted stone sample before and after the treatment (Fig. 9). The final ranking of the adopted six cleaning systems based on their efficiency in removing B-72 is presented in (Fig. 10).

Non-volatile hydrogel residues detection

Characteristic peaks of PVA–B/AG blend hydrogel were absent in all the r-FTIR collected spectra from the samples after the removal process, suggesting that the hydrogel left no residues (within the detection limits of r-FTIR). Iodine-potassium iodide (Lugol's solution) has the ability to stain PVA polymers dark red [65]. Thus, 1% of this solution was used to treat the painted surfaces after B-72 removal by the PVA–B/AG blend. Since there was no color change, the absence of hydrogel residues on the treated surfaces could be confirmed in this manner. These observations were confirmed by the examination under the microscope. It is noteworthy that the residual detection of hydrogels depends on the sensitivity of the techniques used for that purpose. For instance, Angelova et al. [66] used inductively coupled plasma mass spectrometry to track the presence of boron after treatment. To detect residues of the PVA–B system, it was tagged with fluorescein. In the same context, Carretti et al. [24] and Bonelli et al. [67] used FTIR to investigate the absence of residues from PVA–B and polyvinyl alcohol/pyrrolidone gels on some treated surfaces. In all the aforementioned studies no gel residues were detected. However, Riedo et al. [32] detected micro-residues of polyvinyl alcohol/polyethylene oxide (PVA/PEO) gel

Fig. 6 Quantitative results of r-FTIR analyses and the B-72 removal relative efficiency of the six cleaning systems
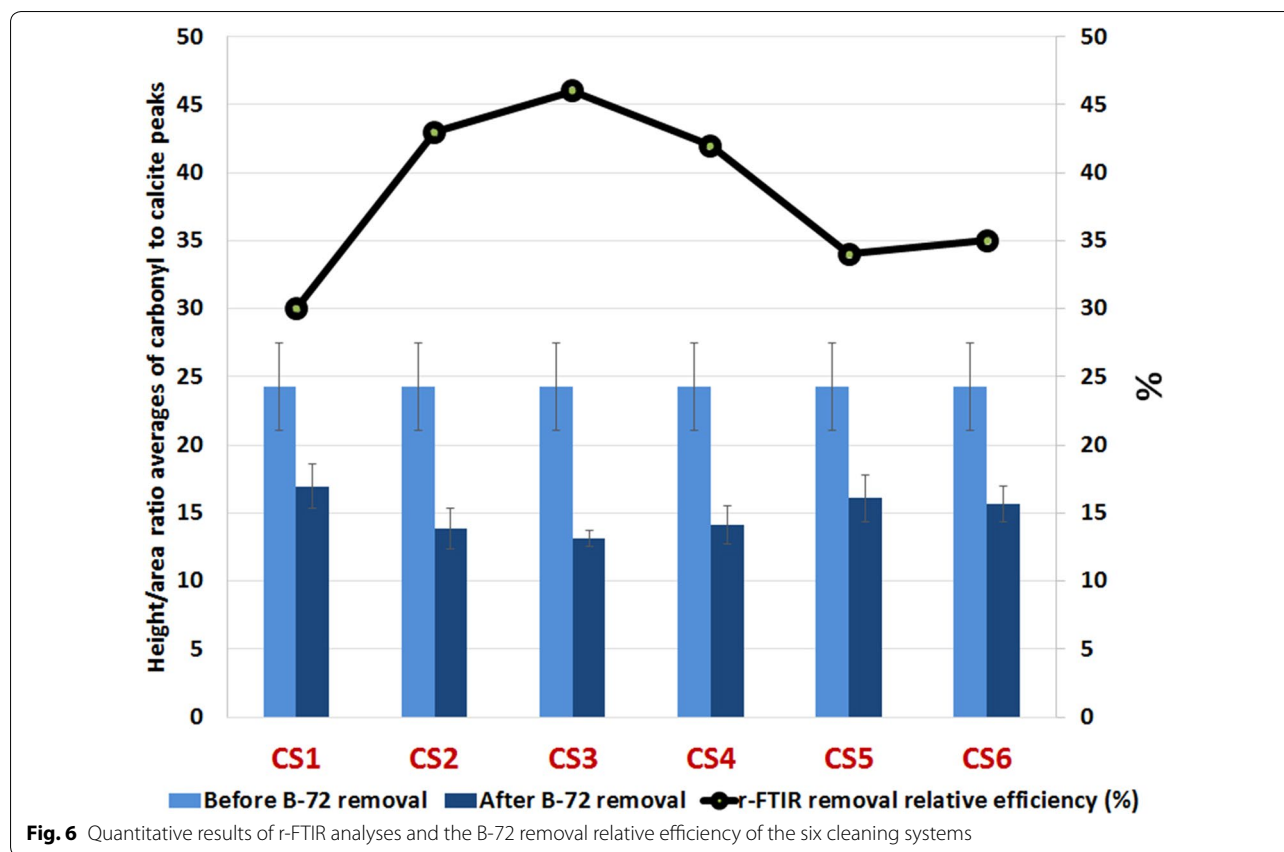
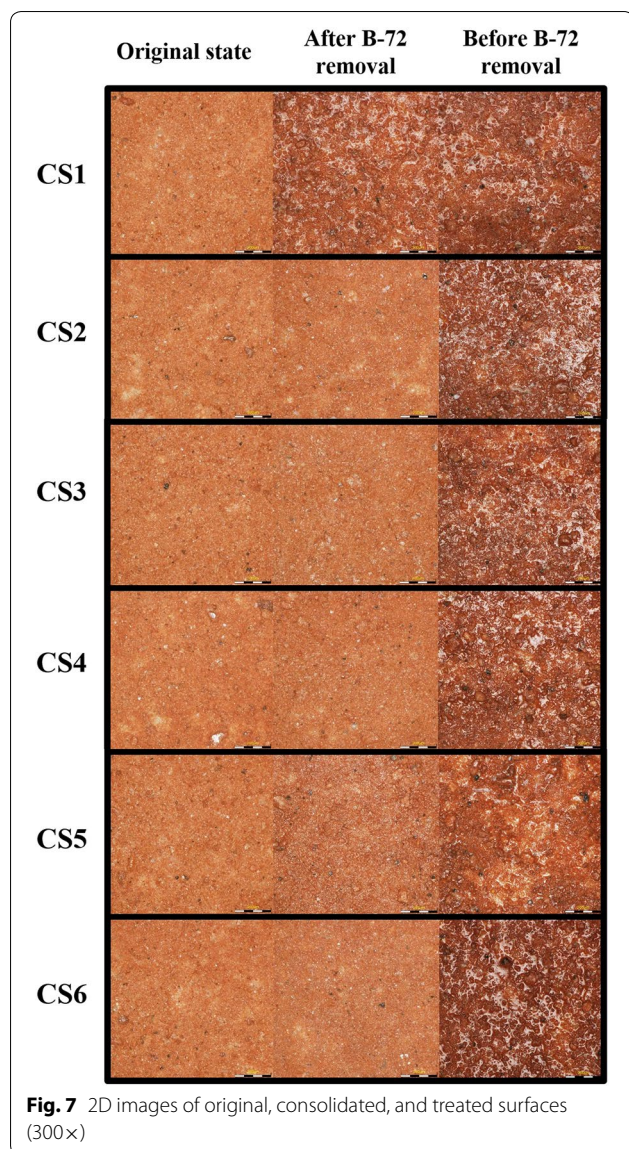by pyrolysis–gas chromatography–mass spectrometry where FTIR spectroscopy was incapable of detecting them.

Furthermore, the analyzed samples, treated with CS5 and CS6, showed none of the characteristic IR peaks of SDS. However, the results of CA measurement indicate the presence of micro-residues.

Field tests

The Temple of Seti I (1306–1290 BC) is a unique architectural landmark that is situated in Abydos (Middle Egypt) and is dated to the 19th Dynasty. Ramesses II (1290–1224 BC) completed the temple after the death of his father Seti I (Fig. 11). The temple is characterized by its highly quality reliefs that are quite observable in the small carved items and hieroglyphs [68, 69]. The paint layers were executed with the gum tempera technique where Arabic gum was used as a binder. The paint layers were either applied directly on the stone or on a plaster layer. The pigments Egyptian blue and green were used to render the blue and green parts of the composition while ochres were used for the red and yellow areas [70–72]. In undocumented previous conservation treatment campaigns, some of the wall paintings were consolidated with an organic polymer. The consolidation left behind a very glossy surface and due to deterioration, the consolidant turned dark and yellow. In addition, these thick layers of the consolidant changed the hydrophobicity of the surface of the wall paintings. It is worth noting that there were several attempts to study the water level in the Osireion building behind the temple which caused changes in the groundwater level under the temple. During these efforts, water was pumped from the Osireion and a number of wells located in different places in/around the temple [73, 74]. Due to this, water rose through capillary action into the walls of the temple where it evaporated during periods of elevated temperature. These cycles of wetting and drying of the walls may have contributed, together with the hydrophobic character of the consolidated paintings, to the detachment of some parts of the painted plasters. This phenomenon is obvious in the wall paintings of the second hypostyle hall such as the suckling scene of Seti I by the goddess Mut (arrow no. 1 in Figs. 11c, 12).

The PVA–B/AG hydrogel were prepared in the lab a day before usage and were packed in sealed plastic bags and then stored in a fridge. The concentrations were PVA 3% and AG 1% in addition to the reported concentration of CS3 (Table 1). The hydrogel was employed to remove the deteriorated consolidant from different test

Al-Emam *et al. Herit Sci*   (2019) 7:22

Page 12 of 18

Fig. 7 2D images of original, consolidated, and treated surfaces (300×)
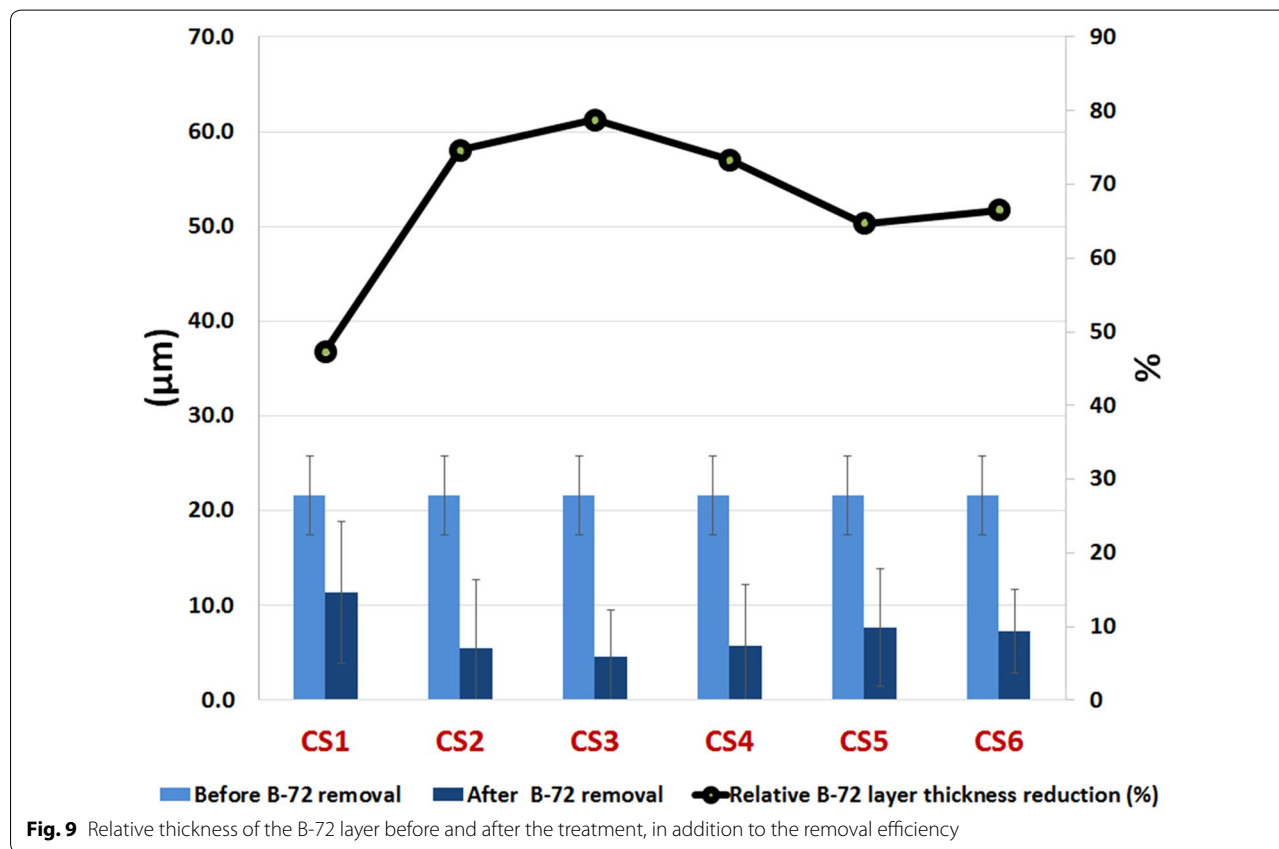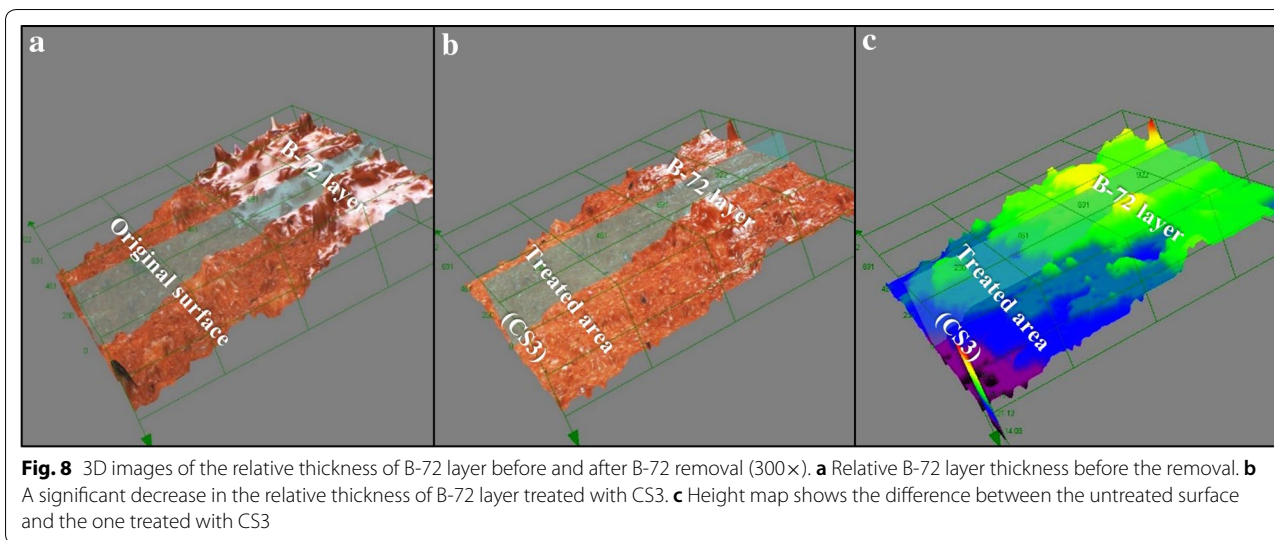
areas in a wall painting in the Chapel of Osiris (arrow no. 2 in Fig. 11c). It is obvious that the wall painting suffers from severe abrasions (scratches) spread over the paint layer (Fig. 13a, b). The hydrogels were applied on the surface with gentle pressure and they were easily able to adapt to the structure of the reliefs. They were covered with plastic sheets to hinder evaporation of the liquids. Two contact times were chosen for the hydrogel application; 1 and 3 h. After this period, the gel was removed and the paint surface gently treated with a dry cotton swab to remove the dissolved consolidant. After the treatment, the glossy and dark aspect of the surface had disappeared and the treated areas showed the original matte surface, which characterizes ancient Egyptian wall paintings, without any visible damage to the paint layer. Both contact times were sufficient

to dissolve and remove the consolidant in the selected test areas (Fig. 13c, d). In addition, one of the already used pieces of the hydrogel was employed for a second application on another test area; also here, it managed to remove the consolidant. The color of the hydrogel pieces changed after they were removed from the wall painting, becoming slightly yellowish while initially being whitish.

Conclusions

The PVA–B/AG blend hydrogel proved to be suitable for removing deteriorated B-72 from painted surfaces with different porosities. This new blend has the potential to retain the cleaning systems into its 3D network and release them consistently to painted surfaces. Cleaning systems may change the appearance of the blend depending on the miscibility of the solvents incorporated and their concentration. The PVA–B/AG hydrogel has good workability as it can be easily shaped as desired as well as simply applied and removed from painted surfaces by means of forceps. In the case of surfaces with reliefs, the blend is flexible enough to adapt to the 3D form of their structure. Besides, it can be applied in a vertical position which is suitable for wall paintings treatments. The blend has self-healing properties and its shape remains stable in long contact time without flowing over the surface. It was verified that PVA–B/AG hydrogel left no detectable residues on the treated surfaces using different investigating methods such as optical microscopy, r-FTIR, and Lugol's solution test. However, in special cases, it possibly leaves residues in case it is applied on a highly porous surface with long contact time. Thus, conservators should implement preliminary tests to determine the appropriate contact time for hydrogel application especially in polymer removal. On the one hand, short contact time may cause partial dissolving of B-72 polymer which becomes tacky and this will probably lead to damaging fragile paint layers during cotton swab clearance. On the other hand, long contact time may cause the hydrogel to dry out and adhere to the consolidated surface by the re-dried B-72 layer. Depending on the surface porosity, the hydrogel can be reused for several applications which lowers the cost of the conservation treatments.

Regarding the tested cleaning systems, CS3, composed of MEK/1-PeOH (10/10%), was the most effective one in removing the B-72 polymer in addition to restoring the color to a state close to that of the original surface. According to the adopted evaluation methods, the differences in the efficiency of CS2 and CS4 were small. The results of the two NSFs revealed low efficiency in removing B-72. These results are contradictory to the information provided in literature about the high efficiency of NSFs in removing a wide range organic polymers

Fig. 8 3D images of the relative thickness of B-72 layer before and after B-72 removal (300×). **a** Relative B-72 layer thickness before the removal. **b** A significant decrease in the relative thickness of B-72 layer treated with CS3. **c** Height map shows the difference between the untreated surface and the one treated with CS3

Fig. 9 Relative thickness of the B-72 layer before and after the treatment, in addition to the removal efficiency

[29, 30, 75]. In several case studies, NSFs were delivered to the deteriorated surface via various systems such as: cellulose pulp poultices, hydrophobically modified hydroxyethylcellulose (hmHEC) and poly(2-hydroxyethyl methacrylate)/polyvinylpyrrolidone pHEMA/PVP gel [41, 76, 77]. This low efficiency, in our study, can be attributed to the fact that they were used at a concentration level of 25% and consequently they were diluted by the water content of the hydrogel. Thus, it is possible that the structure of the NSFs may have modified and that the cleaning action was carried out by free solvents released by the system. However, CS6 was partially effective and
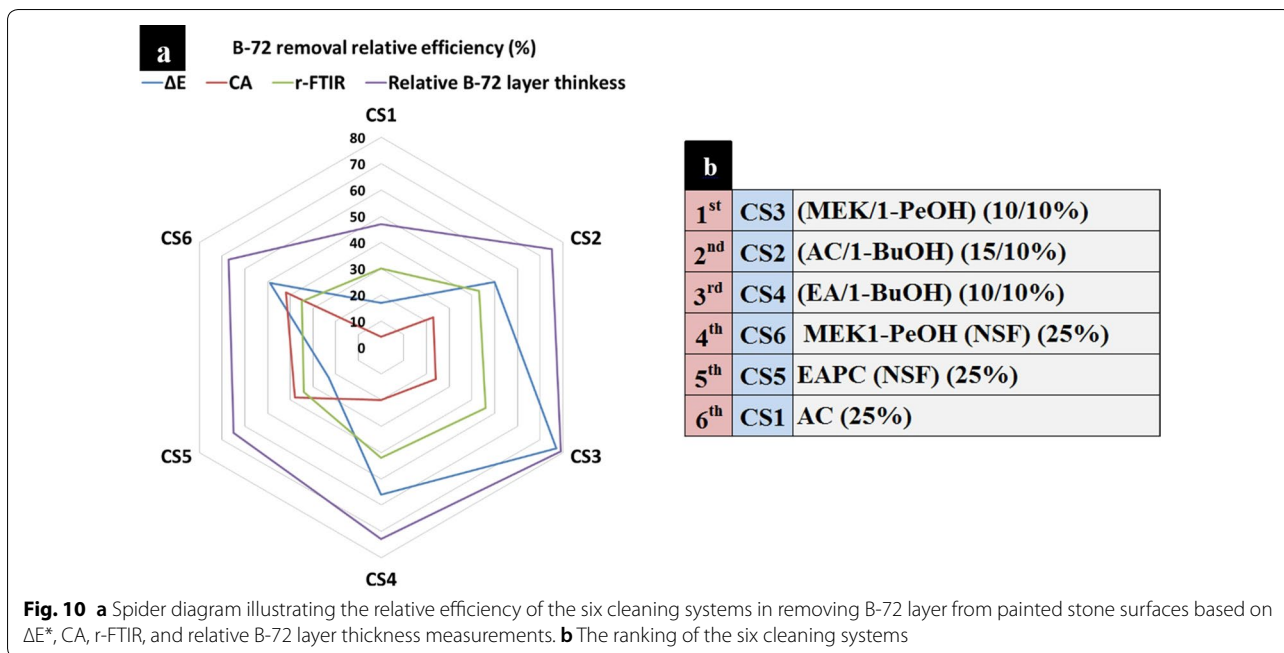
Fig. 10 a Spider diagram illustrating the relative efficiency of the six cleaning systems in removing B-72 layer from painted stone surfaces based on ΔE*, CA, r-FTIR, and relative B-72 layer thickness measurements. **b** The ranking of the six cleaning systems

Fig. 11 a Location of the temple of Seti I in Egypt. **b** View of the temple. **c** Plan of the temple. The arrows locate the wall paintings referred to in the text

better than C5 particularly from a colorimetric point of view. Acetone was effective in dissolving non-deteriorated B-72 but it lost this efficiency against deteriorated B-72.

It appears that there is no accurate correlation between a good B-72 removal from painted surfaces and colorimetric measurements because some of the cleaning systems partially removed B-72 though they provided good colorimetric results as in the case of CS6. Thus, colorimetric measurements should be combined with other evaluating methods to reach conclusive conclusions. Furthermore, CA measurement results reflected the removal efficiency of CS1–CS4 that are composed of pure solvents; however, it may be unreliable with NFSs cleaning systems that contain surfactants. The possibility of the presence of any surfactant remains on the surface after the treatment would influence the delivered water drops surface tension and thusly the CA results. Both r-FTIR and 3D microscope are beneficial tools for the qualitative and quantitative evaluation of the removal efficiency of B-72 besides the detection of gel residues after the treatment process.
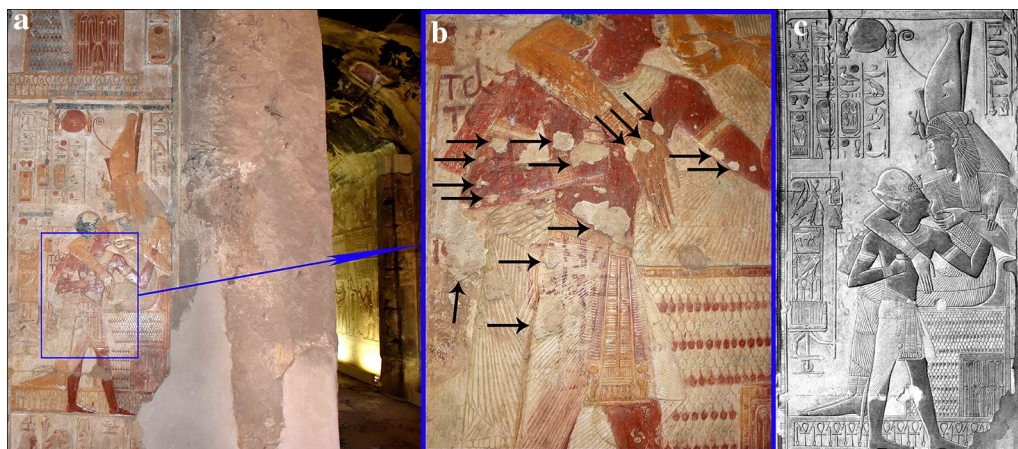
Fig. 12 a A masterpiece scene of the infant Pharao Seti I being suckled by the divine mother goddess Mut. It is located at the second hypostyle hall, west wall between the chapels of Amen-Re and Re-Harakate. **b** The detached painted plaster layer (indicated by black arrows) caused by the thick glossy consolidant layer. **c** The same scene in a black and white photograph of the 1930s reveals the changes occurred since then to the wall painting because of deterioration [78]
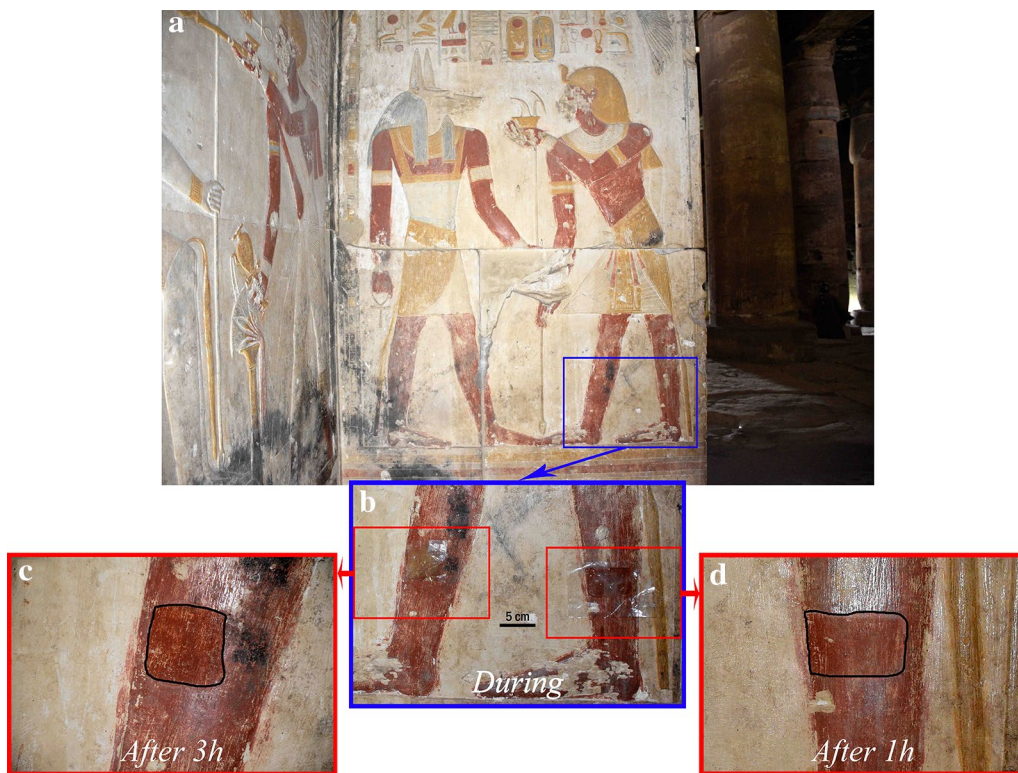

Fig. 13 a Wall painting showing Pharao Seti I presenting incense before the god Wepwawet. The chosen area for the test, before hydrogel application, is indicated by the blue rectangular. This scene is located in the chapel of Osiris, east wall, north side. **b** The PVA–B/AG blend hydrogel, loaded with CS3, during application on two different areas and covered with plastic sheets. **c**, **d** The treated areas, under raking light, after the removal of the consolidant layer (contact times are 3 h and 1 h respectively). The glossy effect of the consolidant disappeared and that the matte appearance of the surface was restored (areas within the black line). The paint layer was not damaged during the removal and all visible scratches are part of the original state of the wall painting

In the end, the PVA–B/AG blend hydrogel, loaded with CS3, was effective in removing deteriorated consolidant layers from a wall painting from the temple of Seti I at Abydos, Egypt. The treatment restored the original matte surface and removed the yellowed/dark aspect of the surface caused by the consolidant. Moreover, the treatment caused no damage to the original paint layer.

Further investigations of PVA–B/AG blend hydrogel are ongoing to understand its characteristics and its ability in cleaning other types of deposits such as aged varnishes and soot from wall painting surfaces.

Abbreviations
ΔE^*: color difference; 1-BuOH: 1-butanol; 1-PeOH: 1-pentanol; AC: acetone; AG: agarose; B-72: Paraloid® B72; CA: contact angle; EA: ethyl acetate; hmHEC: hydrophobically modified hydroxyethylcellulose; HVPD: high viscous polymeric dispersion; MEK: methyl ethyl ketone; NSF: nanostructured fluid; PC: propylene carbonate; PEO: polyethylene glycol; pHEMA/PVP: poly(2-hydroxyethyl methacrylate)/polyvinylpyrrolidone; PVA: polyvinyl alcohol; PVA–B: polyvinyl alcohol–borax; r-FTIR: reflectance FTIR; SDS: sodium dodecyl sulfate.

Authors' contributions
EA performed the tests and measurements, in addition to preparing the hydrogels for the field tests. The first draft of the manuscript was prepared and written by EA. KJ and JC contributed to the strategy of the research as well as writing and revising the manuscript. AM carried out the field tests. All authors read and approved the final manuscript.

Author details
[1] Department of Conservation, Faculty of Archaeology, Sohag University, Sohag 82524, Egypt. [2] Department of Archaeological Conservation, Ministry of Antiquities, Sohag, Egypt. [3] AXES, Department of Chemistry, University of Antwerp, Groenenborgerlaan 171, 2020 Antwerp, Belgium. [4] Heritage & Sustainability, Heritage Department, Faculty of Design Sciences, University of Antwerp, Blindestraat 9, 2000 Antwerp, Belgium.

Competing interests
The authors declare that they have no competing interests.

Availability of data and materials
All the data are available within the manuscript.

Publisher's Note
Springer Nature remains neutral with regard to jurisdictional claims in published maps and institutional affiliations.

References
1. Mora P, Mora L, Philippot P. Conservation of wall paintings. London: Butterworths; 1984.
2. Baglioni P, Chelazzi D, Giorgi R. Nanotechnologies in the conservation of cultural heritage: a compendium of materials and techniques. Dordrecht: Springer; 2015.
3. Baglioni P, Giorgi R, Chelazzi D. The degradation of wall paintings and stone: specific ion effects. Curr Opin Colloid Interface Sci. 2016;23:66–71.
4. Del Lama EA, Tirello RA, Andrade FRDd, Kihara Y. Study of mural paintings by Fulvio Pennacchi in São Paulo City by mineralogical techniques. Acad Bras Ciênc. 2009;81(1):115–26.
5. Abd El-Tawab N, Mahran A, Gad K. Conservation of the mural paintings of the Greek Orthodox Church Dome of Saint George, Old Cairo-Egypt. Eur Sci J. 2015;10(2):324–54.
6. Darwish SS. Evaluation of the effectiveness of some consolidants used for the treatment of the Xixth Century Egyptian cemetery wall painting. Int J Conserv Sci. 2013;4(4):413–22.
7. Wheeler G. Alkoxysilanes and the consolidation of stone. Los Angeles: Getty Conservation Institute; 2005.
8. Matteini M, Rescic S, Fratini F, Botticelli G. Ammonium phosphates as consolidating agents for carbonate stone materials used in architecture and cultural heritage: preliminary research. Int J Archit Heritage. 2011;5(6):717–36.
9. Carretti E, Dei L. Physicochemical characterization of acrylic polymeric resins coating porous materials of artistic interest. Prog Org Coat. 2004;49(3):282–9.
10. Zhang H, Liu Q, Liu T, Zhang B. The preservation damage of hydrophobic polymer coating materials in conservation of stone relics. Prog Org Coat. 2013;76(7):1127–34.
11. Sease C. The case against using soluble nylon in conservation work. Stud Conserv. 1981;26(3):102–10.
12. Horie V. Materials for conservation: organic consolidants, adhesives and coatings. 2nd ed. Amsterdam: Butterworth-Heinemann; 2010.
13. Carretti E, Dei L, Baglioni P. Solubilization of acrylic and vinyl polymers in nanocontainer solutions. Application of microemulsions and micelles to cultural heritage conservation. Langmuir. 2003;19(19):7867–72.
14. Carretti E, Salvadori B, Baglioni P, Dei L. Microemulsions and micellar solutions for cleaning wall painting surfaces. Stud Conserv. 2005;50(2):128–36.
15. Baglioni M, Jàidar Benavides Y, Berti D, Giorgi R, Keiderling U, Baglioni P. An amine-oxide surfactant-based microemulsion for the cleaning of works of art. J Colloid Interface Sci. 2015;440:204–10.
16. Baglioni P, Berti D, Bonini M, Carretti E, Dei L, Fratini E, et al. Micelle, microemulsions, and gels for the conservation of cultural heritage. Adv Coll Interface Sci. 2014;205:361–71.
17. Giorgi R, Baglioni M, Berti D, Baglioni P. New methodologies for the conservation of cultural heritage: micellar solutions, microemulsions, and hydroxide nanoparticles. Acc Chem Res. 2010;43(6):695–704.
18. Natali I, Carretti E, Angelova L, Baglioni P, Weiss RG, Dei L. Structural and mechanical properties of "peelable" organoaqueous dispersions with partially hydrolyzed poly(vinyl acetate)-borate networks: applications to cleaning painted surfaces. Langmuir. 2011;27(21):13226–35.
19. Prati S, Volpi F, Fontana R, Galletti P, Giorgini L, Mazzeo R, et al. Sustainability in art conservation: a novel bio-based organogel for the cleaning of water sensitive works of art. Pure Appl Chem. 2017;90(2):239–51.
20. Baglioni P, Chelazzi D, Giorgi R, Poggi G. Colloid and materials science for the conservation of cultural heritage: cleaning, consolidation, and deacidification. Langmuir. 2013;29(17):5110–22.
21. Angelova LV, Terech P, Natali I, Dei L, Carretti E, Weiss RG. Cosolvent gel-like materials from partially hydrolyzed poly(vinyl acetate)S and borax. Langmuir. 2011;27(18):11671–82.
22. Angelova LV. Gels from borate-crosslinked partially hydrolyzed poly(vinyl acetate)S: characterization of physical and chemical properties and applications in art conservation: Georgetown University; 2013.
23. Carretti E, Grassi S, Cossalter M, Natali I, Caminati G, Weiss RG, et al. Poly(vinyl alcohol)–borate hydro/cosolvent gels: viscoelastic properties, solubilizing power, and application to art conservation. Langmuir. 2009;25(15):8656–62.
24. Carretti E, Natali I, Matarrese C, Bracco P, Weiss RG, Baglioni P, et al. A new family of high viscosity polymeric dispersions for cleaning easel paintings. J Cult Heritage. 2010;11(4):373–80.

Al-Emam *et al. Herit Sci*   (2019) 7:22

Page 17 of 18

25. Carretti E, Bonini M, Dei L, Berrie BH, Angelova LV, Baglioni P, et al. New frontiers in materials science for art conservation: responsive gels and beyond. Acc Chem Res. 2010;43(6):751–60.
26. Angelova L, Carretti E, Berrie BH, Weiss RG. Poly(vinyl alcohol)–borax 'gels': a flexible cleaning option. In: Angelova LV, Ormsby B, Townsend J, Wolbers R, editors. Gels in the conservation of art. London: Archetype Publication; 2017. p. 231–6.
27. Baglioni P, Carretti E, Chelazzi D. Nanomaterials in art conservation. Nat Nanotechnol. 2015;10:287.
28. Duncan TT, Berrie BH, Weiss RG. Soft, peelable organogels from partially hydrolyzed poly(vinyl acetate) and benzene-1,4-diboronic acid: applications to clean works of art. ACS Appl Mater Interfaces. 2017;9(33):28069–78.
29. Chelazzi D, Giorgi R, Baglioni P. Microemulsions, micelles, and functional gels: how colloids and soft matter preserve works of art. Angew Chem Int Ed. 2018;57(25):7296–303.
30. Mastrangelo R, Montis C, Bonelli N, Tempesti P, Baglioni P. Surface cleaning of artworks: structure and dynamics of nanostructured fluids confined in polymeric hydrogel networks. Phys Chem Chem Phys. 2017;19(35):23762–72.
31. Riedo C, Caldera F, Poli T, Chiantore O. Poly(vinylalcohol)-borate hydrogels with improved features for the cleaning of cultural heritage surfaces. Heritage Sci. 2015;3(1):23.
32. Riedo C, Giulia R, Dominque S, Chiantore O. Improved PVA gels for the cleaning of paint surfaces. In: Angelova LV, Ormsby B, Townsend J, Wolbers R, editors. Gels in the conservation of art. London: Archetype Publication; 2017. p. 283–6.
33. Lyons JG, Geever LM, Nugent MJ, Kennedy JE, Higginbotham CL. Development and characterisation of an agar-polyvinyl alcohol blend hydrogel. J Mech Behav Biomed Mater. 2009;2(5):485–93.
34. Sousa AM, Souza HK, Uknalis J, Liu SC, Goncalves MP, Liu L. Electrospinning of Agar/PVA aqueous solutions and its relation with rheological properties. Carbohydr Polym. 2015;115:348–55.
35. Alcântara MTS, Brant AJC, Giannini DR, Pessoa JOCP, Andrade AB, Riella HG, et al. Influence of dissolution processing of PVA blends on the characteristics of their hydrogels synthesized by radiation—part I: gel fraction, swelling, and mechanical properties. Radiat Phys Chem. 2012;81(9):1465–70.
36. Varshney L. Role of natural polysaccharides in radiation formation of PVA–hydrogel wound dressing. Nucl Instrum Methods Phys Res, Sect B. 2007;255(2):343–9.
37. Chiantore O, Lazzari M. Photo-oxidative stability of paraloid acrylic protective polymers. Polymer. 2001;42(1):17–27.
38. Borrelli E. Arc laboratory handbook. Rome: ICCROM; 1999.
39. Teutonico JM. A laboratory manual for architectural conservation. Rome: ICCROM; 1988.
40. Brajer I, Fossé-Le Rouzic M, Shashoua Y, Taube M, Chelazzi D, Baglioni M, et al. The removal of aged acrylic coatings from wall paintings using microemulsions. In: Bridgland J, editor. Icom-Cc 17th triennial conference preprints, Melbourne, 15–19 September 2014. Paris: International Council of Museums; 2014.
41. Baglioni M, Giorgi R, Berti D, Baglioni P. Smart cleaning of cultural heritage: a new challenge for soft nanoscience. Nanoscale. 2012;4(1):42–53.
42. Raudino M, Giamblanco N, Montis C, Berti D, Marletta G, Baglioni P. Probing the cleaning of polymeric coatings by nanostructured fluids: a Qcm-D study. Langmuir. 2017;33(23):5675–84.
43. Raudino M, Selvolini G, Montis C, Baglioni M, Bonini M, Berti D, et al. Polymer films removed from solid surfaces by nanostructured fluids: microscopic mechanism and implications for the conservation of cultural heritage. ACS Appl Mater Interfaces. 2015;7(11):6244–53.
44. Cremonesi P. Surface cleaning? Yes, freshly grated agar gel, please. Stud Conserv. 2016;61(6):362–7.
45. Gulotta D, Saviello D, Gherardi F, Toniolo L, Anzani M, Rabbolini A, et al. Setup of a sustainable indoor cleaning methodology for the sculpted stone surfaces of the Duomo of Milan. Heritage Sci. 2014;2(1):6.
46. Pouli P, Nevin A, Andreotti A, Colombini P, Georgiou S, Fotakis C. Laser assisted removal of synthetic painting-conservation materials using Uv radiation of Ns and Fs pulse duration: morphological studies on model samples. Appl Surf Sci. 2009;255(9):4955–60.
47. Aleix BG, Silvia MO. The removal of Paraloid B-72 coatings with aqueous gelled systems: Roman frescoes from Empúries, Catalonia. In:

48. Carretti E, Giorgi R, Berti D, Baglioni P. Oil-in-water nanocontainers as low environmental impact cleaning tools for works of art: two case studies. Langmuir. 2007;23(11):6396–403.
49. Baglioni M, Jáidar Benavides Y, Desprat-Drapela A, Giorgi R. Amphiphile-based nanofludis for the removal of styrene/acrylate coatings: cleaning of stucco decoration in the Uaxactun archeological site (Guatemala). J Cult Heritage. 2015;16(6):862–8.
50. Grassi S, Carretti E, Pecorelli P, Iacopini F, Baglioni P, Dei L. The conservation of the Vecchietta's wall paintings in the Old Sacristy of Santa Maria Della Scala in Siena: the use of nanotechnological cleaning agents. J Cult Herit. 2007;8(2):119–25.
51. Iwanicka M, Moretti P, van Oudheusden S, Sylwestrzak M, Cartechini L, van den Berg KJ, et al. Complementary use of optical coherence tomography (Oct) and Reflection Ftir spectroscopy for in-situ non-invasive monitoring of varnish removal from easel paintings. Microchem J. 2018;138:7–18.
52. Sun M, Zou J, Zhang H, Zhang B. Measurement of reversible rate of conservation materials based on gel cleaning approach. J Cult Heritage. 2015;16(5):719–27.
53. Schalm O, Storme P, Gambirasi A, Favaro M, Patelli A. How effective are reducing plasma afterglows at atmospheric pressure in removing sulphide layers: application on tarnished silver, sterling silver and copper. Surf Interface Anal. 2018;50(1):32–42.
54. Casadio F, Toniolo L. Polymer treatments for stone conservation: methods for evaluating penetration depth. J Am Inst Conserv. 2004;43(1):3–21.
55. Hein A, Karatasios I, Mourelatos D. Byzantine wall paintings from Mani (Greece): microanalytical investigation of pigments and plasters. Anal Bioanal Chem. 2009;395(7):2061–71.
56. Bikiaris D, Daniilia S, Sotiropoulou S, Katsimbiri O, Pavlidou E, Moutsatsou AP, et al. Ochre-differentiation through micro-Raman and micro-Ftir spectroscopies: application on wall paintings at Meteora and Mount Athos, Greece. Spectrochim Acta A Mol Biomol Spectrosc. 2000;56(1):3–18.
57. Genestar C, Pons C. Earth pigments in painting: characterisation and differentiation by means of Ftir spectroscopy and SEM-EDS Microanalysis. Anal Bioanal Chem. 2005;382(2):269–74.
58. Popescu C-M, Simionescu BC. Structural study of photodegraded acrylic-coated lime wood using Fourier transform infrared and two-dimensional infrared correlation spectroscopy. Appl Spectrosc. 2013;67(6):606–13.
59. Chércoles Asensio R, San Andrés Moya M, de la Roja JM, Gómez M. Analytical characterization of polymers used in conservation and restoration by Atr-Ftir spectroscopy. Anal Bioanal Chem. 2009;395(7):2081–96.
60. Favaro M, Mendichi R, Ossola F, Simon S, Tomasin P, Vigato PA. Evaluation of polymers for conservation treatments of outdoor exposed stone monuments. Part II: photo-oxidative and salt-induced weathering of acrylic–silicone mixtures. Polym Degrad Stab. 2007;92(3):335–51.
61. Chaudhary JP, Kholiya F, Vadodariya N, Budheliya VM, Gogda A, Meena R. Carboxymethylagarose-based multifunctional hydrogel with super stretchable, self-healable having film and fiber forming properties. Arab J Chem. 2018. https://doi.org/10.1016/j.arabjc.2017.12.034.
62. Spoljaric S, Salminen A, Luong ND, Seppälä J. Stable, self-healing hydrogels from nanofibrillated cellulose, poly(vinyl alcohol) and borax via reversible crosslinking. Eur Polym J. 2014;56:105–17.
63. Trivedi TJ, Srivastava DN, Rogers RD, Kumar A. Agarose processing in protic and mixed protic–aprotic ionic liquids: dissolution, regeneration and high conductivity, high strength ionogels. Green Chem. 2012;14(10):2831–9.
64. Viana RB, da Silva ABF, Pimentel AS. Infrared spectroscopy of anionic, cationic, and zwitterionic surfactants. Adv Phys Chem. 2012;2012:14.
65. Schellmann NC, Taylor AC. Establishing the fracture properties of delaminating multilayered decorative coatings on wood and their changes after consolidation with polymer formulations. J Mater Sci. 2015;50(7):2666–81.
66. Angelova LV, Berrie BH, de Ghetaldi K, Kerr A, Weiss RG. Partially hydrolyzed poly(vinyl acetate)–borax-based gel-like materials for conservation of art: characterization and applications. Stud Conserv. 2015;60(4):227–44.
67. Bonelli N, Poggi G, Chelazzi D, Giorgi R, Baglioni P. Poly(vinyl alcohol)/poly(vinyl pyrrolidone) hydrogels for the cleaning of art. J Colloid Interface Sci. 2019;536:339–48.

Angelova LV, Ormsby B, Townsend J, Wolbers R, editors. Gels in the conservation of art. London: Archetype Publication; 2017. p. 363–5.

68. Bunson MR. Encyclopedia of Ancient Egypt. Revised edition ed. New York: Facts on File, Inc; 2002.
69. Wilkinson RH. The complete temples of Ancient Egypt. New York: Thomas & Hudson; 2000.
70. Al-Emam EA, El-Gohary M, Abd El Hady M. Investigations of mural paintings of Seti I and Ramesses Ii Temples at Abydos-Egypt. Int J Conserv Sci. 2014;5(4):421–34.
71. Al-Emam EA, El-Gohary M, Abd El Hady M. The paint layers of mural paintings at Abydos Temples-Egypt: a closer look at the materials used. Mediterr Archaeol Archaeom. 2015;15(3):113–21.
72. Helmi FM, Attia HR. Characterization and conservation of Seti-I Temple Stone, Abydous, Upper Egypt. In: Riederer J, editor. Proceedings of the 8th international congress on deterioration and conservation of stone. vol. 2. Berlin: Möller Druck und Verlag; 1996. p. 1123–36.
73. Parizek A, Abdel Moneim A, Fantle M, Westerman J, Issawi B. Isotopic data: implications for the source(S) of Osireion groundwater, Abydos, Egypt. Egypt J Archaeol Restor Stud. 2011;1(1):61–72.
74. Zaghloul E, Elbeih S. Using remote sensing and Gis techniques to monitor the geoenvironmental changes at Abydos Area, Sohag, Egypt. In: Efe R, Öztürk M, editors. Tourism. Environment and ecology in the Mediterranean Region Cambridge: Cambridge Scholars Publishing; 2014. p. 33–45.
75. Baglioni M, Montis C, Chelazzi D, Giorgi R, Berti D, Baglioni P. Polymer film dewetting by water/surfactant/good-solvent mixtures: a mechanistic insight and its implications for the conservation of cultural heritage. Angew Chem Int Ed. 2018;57(25):7355–9.
76. Carretti E, Fratini E, Berti D, Dei L, Baglioni P. Nanoscience for art conservation: oil-in-water microemulsions embedded in a polymeric network for the cleaning of works of art. Angew Chem Int Ed. 2009;48(47):8966–9.
77. Baglioni M, Domingues JAL, Carretti E, Fratini E, Chelazzi D, Giorgi R, et al. Complex fluids confined into semi-interpenetrated chemical hydrogels for the cleaning of classic art: a rheological and SAXS study. ACS Appl Mater Interfaces. 2018;10(22):19162–72.
78. Calverley AM, Broome MF. The Temple of King Sethos I at Abydos. London: The Egypt Exploration Society; 1933–1958.